# Photostop: Production of Zero-Velocity Molecules by Photodissociation in a Molecular Beam

Eckart Wrede, Alexandre Trottier, David Carty

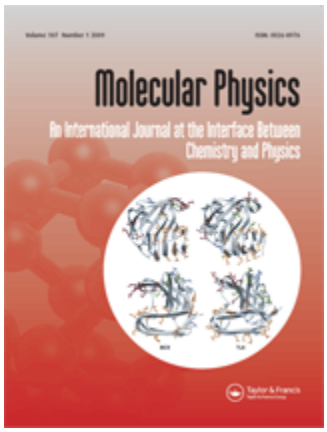


# Photostop: Production of Zero-Velocity Molecules by Photodissociation in a Molecular Beam

| | |
|---|---|
| Journal: | *Molecular Physics* |
| Manuscript ID: | TMPH-2010-0448.R1 |
| Manuscript Type: | Full Paper |
| Date Submitted by the Author: | 08-Dec-2010 |
| Complete List of Authors: | Wrede, Eckart; Durham University, Chemistry<br>Trottier, Alexandre; Durham University, Chemistry<br>Carty, David; Durham University, Chemistry |
| Keywords: | cold molecules, deceleration, trapping, photodissociation |
| | |
| Note: The following files were submitted by the author for peer review, but cannot be converted to PDF. You must view these files (e.g. movies) online. | |
| source files.zip | |

*Molecular Physics*
Vol. 00, No. 00, Month 200x, 1–9

RESEARCH ARTICLE

# *Photostop: Production of Zero-Velocity Molecules by Photodissociation in a Molecular Beam*

Alexandre Trottier[a†], David Carty[ab] and Eckart Wrede[a*]

[a] *Department of Chemistry, Durham University, South Road, Durham, DH1 3LE, U.K.*
[b] *Department of Physics, Durham University, South Road, Durham, DH1 3LE, U.K.*

(*November 18th, 2010*)

Photostop is an accessible ~~, impulsive deceleration~~ technique capable of producing atoms or molecules at a standstill in the laboratory frame. Starting with a $NO_2$/Xe molecular beam with a mean velocity of 415 m s$^{-1}$ and a longitudinal translational temperature of 6 K, $NO_2$ molecules are photodissociated to yield NO($X^2\Pi_{3/2}, v = 0, J = 1.5$) fragments with a recoil speed equal to the molecular beam speed. The fraction of NO fragments that recoil opposite to the molecular beam are produced with a 6 K longitudinal velocity distribution centred at zero. The NO molecules are allowed to "evaporate" from the probe volume by waiting for 10 $\mu$s and the molecules left behind are probed with a translational temperature of 1.6 K along the molecular beam axis and an estimated density of $10^7$ cm$^{-3}$ per quantum state. ~~Starting from a 300 K thermal sample with a mean velocity of zero, we have cooled a mixture of $NO_2$ and Xe to a translational temperature of 6 K in a supersonic molecular beam with a mean velocity of 415 m s$^{-1}$. We have photodissociated the $NO_2$ to produce NO($X^2\Pi_{3/2}, v = 0, J = 1.5$) molecules such that the recoil energy of the NO molecules re-centres the mean velocity of a subset of the NO fragments to zero while maintaining a temperature of 6 K. We have "evaporated" the NO molecules over a period of 10 $\mu$s leaving a fraction behind at 1.6 K and at an estimated density in excess of $10^7$ cm$^{-3}$ per quantum state.~~ Through the choice of suitable precursors, the photostop technique has the potential to extend the list of atoms and molecules that can be slowed or trapped. It should be possible to accumulate density in a trap through consecutive loading of multiple pulses.

**Keywords:** cold molecules; deceleration; trapping; photodissociation.

## 1. Introduction

The growth over the last decade in the number of experiments designed to create ground state molecules at cold (< 1 K) and ultracold (< 1 mK) temperatures is a direct result of the wide-ranging impact expected from the field. It is anticipated that ensembles of ultracold polar molecules will find many applications due to the possibility that their long-range dipolar interactions can be controlled. Such applications include controlled molecular dynamics, tests of fundamental physical laws, quantum information processing and quantum simulators [1].

Molecular collisions and chemical reactions depend sensitively on the ~~mutual~~ interactions between the molecules. At cold and ultracold temperatures, the collision energy can be ~~is~~ similar to the Stark and Zeeman shifts experienced by the molecules in external fields. Therefore, by applying a tailored external electrical or magnetic field, molecular interactions can be controlled to enhance or suppress specific outcomes of a chemical reaction via the fine-tuning of scattering resonances [2]. The long interrogation times and rich internal structure afforded by trapped ultracold molecules offer inherent advantages for measurements that require ultra-high precision. For example, the determination of the dipole moment of the electron would test for time-reversal symmetry violation [3] and the determination of a time variation of fundamental constants would test for the equivalence principle of general relativity [4]. Ultracold polar molecules that have been trapped in optical lattices could be made to form an adjustable network of variably-interacting quantum bits

†Current address: AECL Chalk River Laboratories, Deep River, ON, K0J 1J0, Canada.
*Corresponding author. Email: eckart.wrede@durham.ac.uk

ISSN: 0040-5167 print/ISSN 1754-2278 online

DOI: 10.1080/0040516YYxxxxxxxx
http://www.informaworld.com

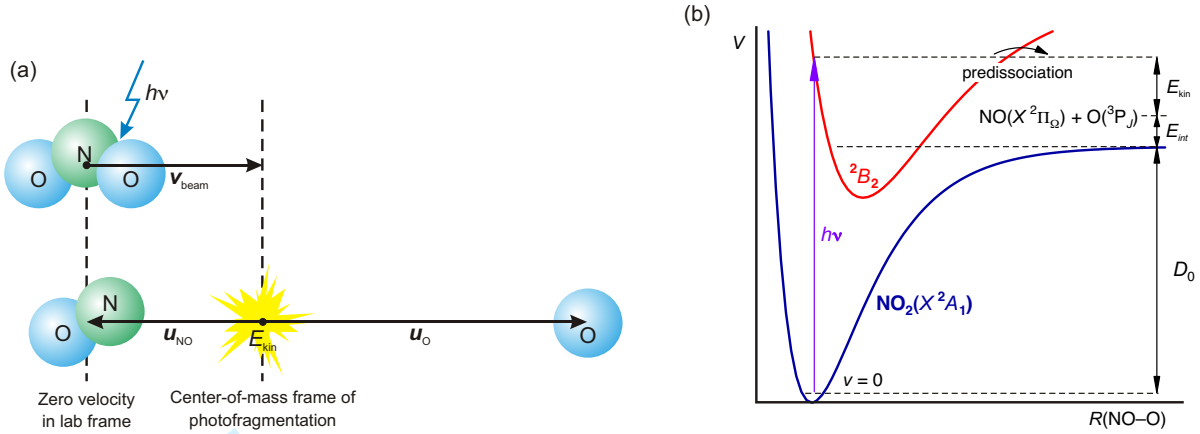


Figure 1. (Colour online) (a) Schematic outline of the photostop technique. The recoil velocity of NO fragments, $\boldsymbol{u}_{\mathrm{NO}}$, from the photodissociation of $NO_2$ molecules cancels the velocity of the molecular beam, $\boldsymbol{v}_{\mathrm{beam}}$. Therefore, NO molecules are produced with zero velocity in the laboratory frame while the oxygen co-fragments are accelerated. (b) Schematic diagram of the $NO_2$ potential energy surfaces. Ground state $NO_2$ molecules are photo excited into the $^2B_2$ state which predissociates onto the ground state surface to form $NO(X\ ^2\Pi_\Omega)$ molecules and $O(^3P_J)$ atoms. By tuning the photon energy, $h\nu$, the total kinetic energy, $E_{\mathrm{kin}}$, released by the photodissociation process can be adjusted for given total internal energy, $E_{\mathrm{int}}$, of both photofragments.



(qubits) where it would be possible to engineer fast logic gates for quantum information processing [5]. Furthermore, such a network could be adjusted to act as a quantum simulator for any fully quantum many-body system for solving problems in condensed matter physics that are intractable using traditional computational methods and hardware [6].

To date, the only polar molecules that have been produced in their rovibronic ground states at ultracold temperatures are KRb [7], RbCs [8] and LiCs [9], which were formed by associating ultracold atoms. The technique is thus far limited to alkali-alkali molecules, which do not possess a magnetic moment, a desirable property for applications. In a promising development, it was shown that it may be possible to laser cool SrF directly to ultracold temperatures due to its unique energy level structure [10]. However, for many applications, a variety of species at ultracold temperatures and high densities is required. Potentially, the ~~The~~ most versatile approach is to sympathetically cool trapped *cold* polar molecules into the ultracold regime using ultracold atoms as a refrigerant [11]. Therefore, the initial production of high densities of a variety of cold molecular species remains a major challenge in the field.

A variety of techniques have been developed for the production of cold molecules [12–15] ~~[12–14]~~ with buffer gas cooling and Stark deceleration being amongst the established leaders in the field [16, 17]. Each technique has its own strengths and technical challenges. Therefore, it is important to continue exploring new complementary techniques with the aim of addressing the challenges of the field, *e.g.* increasing densities or expanding the list of cold species in light of new applications.

In 2007, Matthews *et al.* [18] proposed that cold oxygen atoms could be made from $NO_2$ molecules with zero mean-velocity in the laboratory frame by a method that we are going to refer to ~~dub here~~ as photostop. The photostop method is based on the controlled breaking of one chemical bond (NO–O bond in the proposed case), via photodissociation, in a precursor molecule initially cooled in a supersonic molecular beam. The result is an atomic or molecular fragment that recoils with a velocity that cancels out the initial velocity of the precursor molecule in the beam, $v_{\mathrm{beam}}$, as illustrated in Figure 1(a). Recently, Zhao *et al.* [19] showed in an ion imaging experiment that the mean velocity of the $NO(^2\Pi_{1/2}, v = 1, J \sim 8.5)$ molecular fragment, following the photodissociation of $NO_2$ at the fixed wavelength of 355 nm, could partially cancel the mean molecular beam velocity slowing it from 565 m s$^{-1}$ to 35 m s$^{-1}$. Although they did not mention it in their paper, a small fraction of the NO velocity distribution almost certainly encompassed zero-velocity and they were able to observe NO molecules of indeterminate velocity up to 300 ns after the photodissociation event. Unfortunately, for practical reasons, they could not demonstrate the power of the technique as they were unable to meet the exact velocity cancellation condition and their measurements relied on numerical calculations to infer many of the velocities they quoted. However, they demonstrated the viability of the photostop technique. ~~proved that the principle of the photostop technique was sound.~~

In this paper, we have also chosen $NO_2$ as the precursor molecule and conducted experiments where molecule velocities have been measured directly (employing a different ion imaging geometry, as outlined below) and where the velocity matching condition is met exactly by using a tunable dissociation laser. Based on these measurements, we aim to advance the characterisation of the photostop technique and to assess its prospects.

## 2. Photostop technique

As can be seen in Figure 1(b), photon energies, $h\nu$, exceeding the dissociation energy, $D_0$, of the NO–O bond cause the $NO_2$ molecule to fragment into an NO molecule and an oxygen atom. The excess energy, $E_{\rm exc} = h\nu - D_0$, is partitioned between the kinetic and internal energies of the fragments in varying proportions determined by the complex predissociation dynamics [18]. For fragments formed in a given combination of states, the total internal energy, $E_{\rm int}$, is fixed and the total kinetic energy, $E_{\rm kin}$, released is therefore governed only by the photon energy

$$E_{\rm kin} = E_{\rm kin}({\rm NO}) + E_{\rm kin}({\rm O}) = h\nu - D_0 - E_{\rm int}, \tag{1}$$

where $E_{\rm kin}$(NO) and $E_{\rm kin}$(O) are the kinetic energies of the NO and O fragments, respectively. By conservation of momentum, the velocities of the fragments (in the centre-of-mass frame of the photodissociation process) are given by

$$u_{\rm NO} = \sqrt{2\,E_{\rm kin}\cdot\frac{m_{\rm O}}{m_{\rm NO}\,m_{\rm NO_2}}} \tag{2a}$$

$$u_{\rm O} = \sqrt{2\,E_{\rm kin}\cdot\frac{m_{\rm NO}}{m_{\rm O}\,m_{\rm NO_2}}} \tag{2b}$$

where $m_{\rm O}, m_{\rm NO}$ and $m_{\rm NO_2}$ are the respective masses. NO molecules are stopped in the laboratory frame if $\boldsymbol{u}_{\rm NO} = -\boldsymbol{v}_{\rm beam}$ and, from Equations (1) and (2), the wavelength of the photons required is given by

$$\lambda_{\rm NO} = hc\left[\frac{1}{2}\left(\frac{m_{\rm NO}m_{\rm NO_2}}{m_{\rm O}}\right)v_{\rm beam}^2 + D_0 + E_{\rm int}\right]^{-1} \tag{3}$$

Exchanging the masses of NO and O in Equation (3) yields the corresponding wavelength to stop the O fragment.

## 3. Experiment

A schematic diagram of the experiment is shown in Figure 2(a). The molecular beam is formed from a skimmed pulsed (10 Hz repetition rate) supersonic expansion of 1–5% $NO_2$ in 4 bar of Xe, the direction of which defines the $z$-axis of the experiment. The molecular beam is intersected at right angles by two laser beams counter-propagating along the $x$-axis. The first beam is used to photodissociate the $NO_2$ molecules and is generated by a pulsed dye laser tunable in the range of 380–400 nm. The second beam, generated by another pulsed dye laser tunable around 226 nm, is used to ionise NO($X\,^2\Pi$) molecules in a specific rovibrational quantum state using (1 + 1) resonance-enhanced multiphoton ionisation (REMPI) via the $A\,^2\Sigma$ state. The molecular beam and the laser beams intersect at the centre of an ion lens system oriented along the $y$-axis. The resulting $NO^+$ ions are accelerated by the electrostatic field towards a position sensitive imaging detector consisting of a pair of micro-channel plates, a phosphorescent screen and a CCD camera. The ion lens system is designed and operated such that the velocity of the original NO molecule is mapped onto a unique position on the detector, a technique known as velocity mapped ion imaging (VMI) [20]. The detected ion image corresponds to the 2-dimensional projection of the original 3-dimensional velocity distribution of the NO molecules onto the $(v_x, v_z)$ plane. Such a set-up allows the direct measurement of the absolute velocity of both the molecular beam and of the NO fragment molecules, thus allowing us to optimise easily the photostop process.

In order to measure the velocity of the NO molecules in the laboratory frame, the velocity origin, *i.e.* the position on the detector that corresponds to $(v_x, v_z)$ / m s$^{-1}$ = (0, 0), was found ~~to an accuracy of ±1 m s$^{-1}$~~ by recording an ion image of thermal NO bled into the vacuum chamber. Two ~~and locating the centre of the image by fitting it to~~ one-dimensional Maxwell-Boltzmann distributions of the form

$$f(v_x) \propto \exp\left(-\frac{m_{\rm NO}v_x^2}{2kT}\right), \tag{4}$$

were fitted to this image in both the $v_x$ and $v_z$ directions locating its centre with a sub-pixel precision of ±1 m s$^{-1}$. The velocity of the molecular beam was determined from an ion image of the small fraction of "native" NO present in the beam due to the thermal decomposition of the $NO_2$ sample at room temperature. The velocity of the molecular beam was measured to be $v_{\rm beam}$ = 415 m s$^{-1}$ with a full-width-at-half-maximum (FWHM) of 80 m s$^{-1}$, which corresponds to a translational temperature of the $NO_2$ molecules of 6 K.

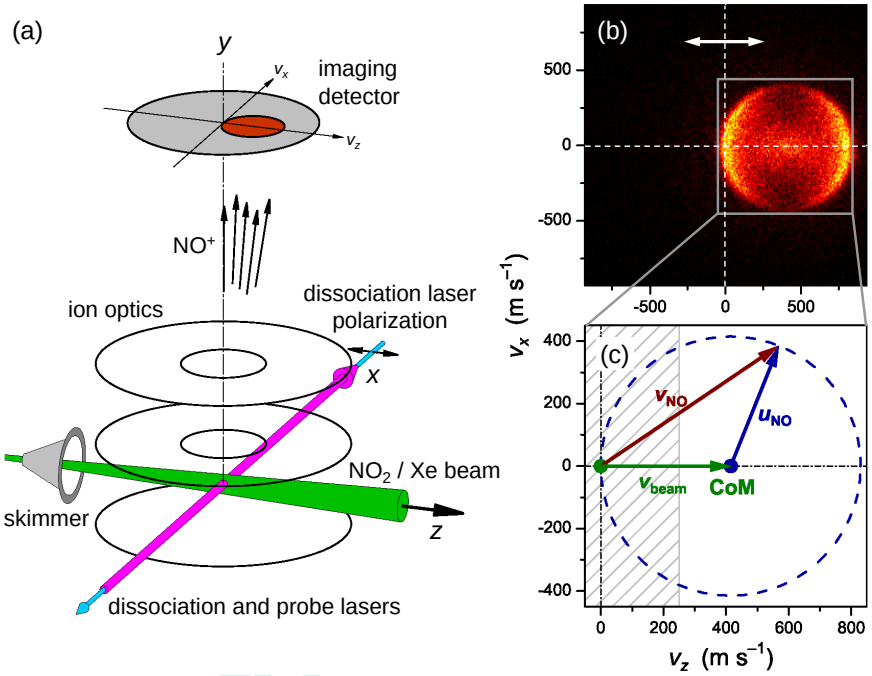


Figure 2. (Colour online) (a) Schematic diagram of the experiment. A pulsed molecular beam of $NO_2$ seeded in Xe is skimmed and intersected at right angles by the photodissociation and probe laser beams. The ionised NO photofragments are accelerated by static electric fields in a velocity map configuration (ion optics) towards a position sensitive detector to image the ions. (b) Velocity mapped ion image of $NO(X\,^2\Pi_{3/2}, v = 0, J = 1.5)$ fragments from the photodissociation of $NO_2$ at 386.4 nm. The image shows the distribution of NO lab velocities projected onto the plane of the molecular and laser beams. The lab velocity origin is indicated by the dotted lines and the arrow indicates the axis of cylindrical symmetry of the dissociation process and the polarisation direction of the dissociation laser. (c) Newton diagram of the photodissociation process in the $(v_z, v_x)$-plane of the experiment. The recoil velocity of the NO fragment, $\boldsymbol{u}_{NO}$, in the centre-of-mass (CoM) frame can lie at any point on the Newton sphere, indicated by the dashed circle, weighted by the anisotropy of the photodissociation process. The NO velocity in the laboratory frame, $\boldsymbol{v}_{NO}$ is the vector sum of the molecular beam velocity, $\boldsymbol{v}_{beam}$, and $\boldsymbol{u}_{NO}$. The necessary kinematic conditions for photostop are met when the Newton sphere intersects the velocity origin. The grey shaded area represents the $|v_z| \leq 250$ m s$^{-1}$ ~~$v_z$~~-velocity acceptance of the probe volume after 1 $\mu$s time delay (*cf.* Figure 3(a)) given an estimated probe beam diameter of 0.5 mm.

There are three sources of NO molecules that can contribute towards signal in the ion image: native NO, present as a background component in the molecular beam; thermal background NO that is not pumped away between gas pulses; and NO produced as a product of the photodissociation. The ratio of spin-orbit excited $NO(^2\Pi_{3/2})$ to ground state $NO(^2\Pi_{1/2})$ molecules present in the beam was measured to be less than 1 : 40, therefore spin-orbit excited NO originates almost exclusively from the $NO_2$ dissociation. Thus, by aiming to photostop spin-orbit excited NO, interference from native NO present in the molecular beam is minimised. All ion images were recorded with an automatic shot-by-shot background subtraction by electronically blocking every second shot from the photodissociation laser. Therefore, any remaining signal from NO present in the background gas in the vacuum chamber is minimised.

Figure 2(b) shows an ion image representing the velocity distribution of NO molecules in the $X\,^2\Pi_{3/2}, v = 0, J = 1.5$ state. The centre of the distribution is offset by the velocity of the molecular beam from the laboratory frame velocity origin, the position of which is illustrated by the cross-hairs. As shown in Figure 2(c), the recoil velocity of the NO fragments, $\boldsymbol{u}_{NO}$, can lie at any point on the Newton sphere. However, the photodissociation of $NO_2$ is strongly anisotropic with a measured $\beta$ parameter of 1.5 which is close to the maximum possible value for a single-photon dissociation process of $\beta_{max} = 2$ (representing a $\cos^2\theta$ angular distribution with respect to the polarisation direction of the dissociation laser beam). By aligning the polarisation of the dissociation light parallel to the molecular beam ($z$) axis, one of the NO fragment angular distribution maxima is pointed towards the velocity origin, as can be seen in Figure 2(b). Finally, the peak of the NO speed distribution was optimally overlapped with the velocity origin by tuning the dissociation laser wavelength to 386.4 nm. Those NO molecules coinciding with the velocity origin are thus photostopped and those that appear on the exact opposite side of the ion image are accelerated to twice the molecular beam speed. According to Equation (3), with $D_0 = 25128.6$ cm$^{-1}$ [21], 386.4 nm corresponds to a NO fragment speed of 418.5 m s$^{-1}$, which equals the molecular beam speed of 415 m s$^{-1}$ to within the nearest pixel on the camera.

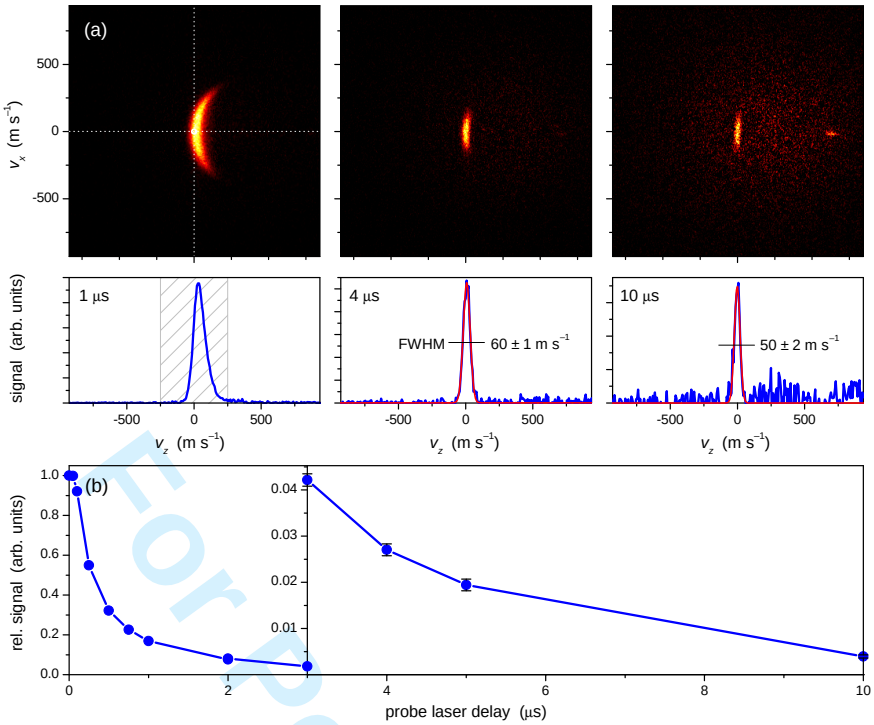





Figure 3. (Colour online) (a) Velocity mapped ion images of NO($X\ ^2\Pi_{3/2}, v = 0, J = 1.5$) fragments from the photodissociation of $NO_2$ under photostop conditions at 386.4 nm and at different time delays between the dissociation and probe lasers. The velocity distribution projected onto the molecular beam axis ($v_z$) is shown underneath each ion image. The grey shaded area represents the $v_z$-velocity acceptance of the probe volume after 1 $\mu$s time delay. One-dimensional Maxwell-Boltzmann velocity distributions are fitted to the profiles at 4 and 10 $\mu$s (red, online), the full-width-at-half-maxima of which are indicated. (b) Decay of the integrated NO signal for each recorded ion image as a function of time delay.

## 4. Stopped molecules

To demonstrate that NO fragments are indeed stopped in the laboratory frame, we have recorded a series of ion images, shown in Figure 3(a), as a function of the time delay between the 5 ns long pulses of the photodissociation and probe lasers. It is clear that molecules remain in the probe laser volume even after 10 $\mu$s. The panels below each of the ion images show the projection of that ion image onto the $v_z$ axis. After 1 $\mu$s delay, it can be seen that those NO fragments that recoil in the same direction as the molecular beam (positive $v_z$) have duely left the probe laser volume. The probe volume is much larger along the $x$ axis than in the other dimensions, therefore, only NO molecules with small $v_y$ and $v_z$ components are detected by the probe laser. On the contrary, molecules with larger $v_x$ components are detected. The grey shaded areas in Fig. 2(c) and Figure 3(a) represent the velocity acceptance of the probe volume after 1 $\mu$s delay. All recoiling NO molecules with velocities that lie within this velocity acceptance appear as a crescent shape in the 1 $\mu$s ion image. The asymmetry on the positive side of the corresponding $v_z$ profile is simply due to the projection of the crescent onto the $v_z$ axis. After a delay of 4 $\mu$s, and subsequently 10 $\mu$s, the ion images appear straighter because the velocity acceptance narrows in both $v_y$ and $v_z$, but not in $v_x$. The corresponding projections are almost symmetrical, thus, a temperature can be assigned by fitting the profiles to Equation (4). We obtain from the measured velocity distributions one-dimensional temperatures of $T = 2.4 \pm 0.1$ K and $1.6 \pm 0.1$ K, for delays of 4 and 10 $\mu$s, respectively, although these include contributions from the electron recoil upon ionisation and from the velocity resolution of the imaging detector. Once these contributions are removed the one-dimensional temperatures are $T = 2.0 \pm 0.1$ K and $1.3 \pm 0.1$ K, respectively.

Figure 3(b) shows the decay of the normalised, integrated NO($X\ ^2\Pi_{3/2}, v = 0, J = 1.5$) signal in each recorded ion image as a function of delay time. The signal decays rapidly in the first microsecond due to NO molecules that recoil in the forward direction of the molecular beam leaving the probe volume. This is followed by a slow decay that represents the remaining slow molecules "evaporating" from the probe volume. After 10 $\mu$s, $0.39 \pm 0.05\%$ of the detected NO fragments present at zero delay remain. The main contribution to the evaporation is due to the velocity spreads of the NO fragments perpendicular to the molecular beam ($\Delta v_x$ and $\Delta v_y$) being large compared to the corresponding velocity acceptances of the probe volume because of the fragment angular distribution, *cf.* Figure 2(b). The remaining contribution to the evaporation is due to the velocity spread of the molecular beam. At a delay of 10 $\mu$s, the FWHM of the $v_z$ velocity

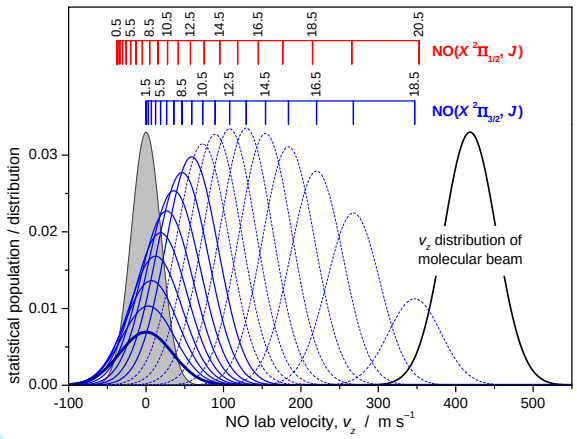


Figure 4. (Colour online) Lab velocities and distributions along the molecular beam axis ($v_z$) of NO fragments produced by photodissociation of $NO_2$ at 386.4 nm. The fitted Gaussian velocity distribution of the $NO_2$ molecular beam (black line) and the velocity acceptance for NO fragments of the probe volume at 10 $\mu$s delay (grey shaded area) are indicated. The central lab $v_z$ velocities of all energetically accessible rotational levels of both ground state spin-orbit components are shown as combs ($X\ ^2\Pi_{1/2}$ red, $^2\Pi_{3/2}$ blue). For the spin-orbit excited NO($^2\Pi_{3/2}$) fragments, the $v_z$ velocity distributions of each rotational level are shown as Gaussians with amplitudes that correspond to their assumed statistical population. Distributions with a significant overlap with the probe velocity acceptance are shown as solid (blue) lines; the distribution of the probed $^2\Pi_{3/2}, J = 1.5$ level is highlighted as a thick solid (blue) line.

acceptance of the probe volume is $\pm 23$ m s$^{-1}$ (see Figure 3(a)) compared to the $\pm 40$ m s$^{-1}$ velocity spread of the molecular beam.

The photon energy used in these experiments is 751 cm$^{-1}$ above the dissociation threshold, which is energetic enough to populate NO rotational levels up to $J = 20.5$ and $J = 18.5$ in the $^2\Pi_{1/2}$ and $^2\Pi_{3/2}$ spin-orbit states, respectively. Although energetically allowed, no evidence of spin-orbit excited O($^3P_{1,0}$) co-fragments was found. Unfortunately, due to the complex dissociation dynamics [18], the state distribution is as yet unknown at the photodissociation energy used and cannot be determined with confidence in our experiment due to the non-linear REMPI detection scheme employed. However, assuming a statistical prior state distribution (which includes the phase space contribution of the recoiling fragments proportional to $\sqrt{E_{\rm kin}}$), we estimate the proportion of NO($^2\Pi_{3/2}, J = 1.5$) to be 0.7%. Figure 4 shows NO $v_z$ lab velocity distributions of the rotational states of the $^2\Pi_{3/2}$ spin-orbit component scaled according to the statistical populations together with the $v_z$ velocity acceptance of the probe volume after 10 $\mu$s. Due to the significant velocity spread of the precursor molecular beam, NO molecules in many rotational states are still within the probe volume. Convoluting all NO lab $v_z$ distributions with the probe velocity acceptance (Gaussian with 45 m s$^{-1}$ FWHM) we estimate that 95% of the NO molecules present in the probe volume are in quantum states $^2\Pi_{1/2}, J = 2.5 - 13.5$ and $^2\Pi_{3/2}, J = 1.5 - 9.5$ at 10 $\mu$s delay. NO molecules in the remaining quantum states are therefore not photostopped. Assuming a $NO_2$ density in the probe volume of $10^{12}$ cm$^{-3}$, and taking into account the losses discussed above (0.7% × 0.39%), we estimate the density of photostopped and probed NO($^2\Pi_{3/2}, J = 1.5$) molecules at 10 $\mu$s delay to be $\approx 3 \cdot 10^7$ cm$^{-3}$. These molecules represent only 2% of all molecules in the probe volume at 10 $\mu$s delay, therefore ~~Including *all* molecules in the probe volume after 10 $\mu$s delay irrespective of their quantum state~~ we estimated the density of *all* photostopped molecules to be about $10^9$ cm$^{-3}$.

## 5. Prospects

The implementation of the photostop technique is relatively simple as it is based on well established knowledge and technology. The technique is economical in its requirements: a molecular beam source; a tunable photodissociation laser; and a suitable laser spectroscopic detection method, *e.g.* laser induced fluorescence. The velocity map ion imaging detection technique is a very effective analytical tool for the success of these experiments because it allows the direct measurement of the molecular beam and photofragment velocities, provided that the ion optics are oriented perpendicular to the molecular beam axis.

The estimated density of stopped molecules in these measurements could be improved. The distance between the nozzle and the laser beams is relatively large at 150 mm. With changes to the experimental setup, the nozzle-to-laser distance could feasibly be reduced to 50 mm, thus increasing the $NO_2$ density by an order of magnitude. Therefore, the density of photostopped NO molecules in all states could be increased to more than $10^{10}$ cm$^{-3}$. However, the ~~The~~ photostop process takes place in the path of the molecular beam.

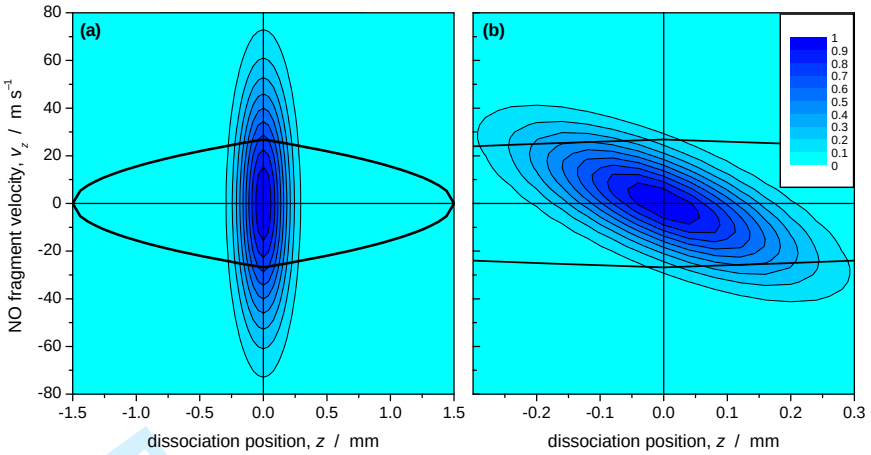


Figure 5. (Colour online) Relative phase-space densities in the direction of the molecular beam $(z, v_z)$ of photostopped NO($^2\Pi_{3/2}, J = 1.5$) molecules. (a) Phase-space density of the source volume using the experimental diameter of the dissociation laser beam ($\approx$ 0.3 mm FWHM) and the velocity spread of the molecular beam (80 m s$^{-1}$ FWHM). The separatrix of the phase-space acceptance of a 1.3 K deep and 5 mm wide quadrupole magnetic trap in anti-Helmholtz configuration is indicated by the thick solid black lines. (b) Phase-space acceptance of the probe laser volume after 10 $\mu$s delay.

Therefore, elastic or inelastic collisions between stopped NO fragments and the carrier gas may remove stopped NO from the probe volume, an effect that will increase with decreasing nozzle-to-laser distances. Following this work, we have conducted experiments to photostop Br atoms using $Br_2$ as a precursor seeded in Kr [22]. We observed photostopped Br atoms at times up to 100 $\mu$s after the photodissociation event, by which time the entire gas pulse has passed through the stopped atoms. Monte Carlo simulations of the photostop process without scattering taken into account reproduce the experimental results excellently suggesting that scattering due to collisions with the carrier gas are not significant in this system. In systems where scattering may be significant, it can be minimised, *e.g.* by mechanically chopping the part of the gas pulse that follows the dissociation laser pulse.

We are currently implementing a magneto-static trap constructed from permanent magnets that will confine photostopped NO($^2\Pi_{3/2}, v = 0, J = 1.5$) molecules in the low field seeking $M_J = 3/2$ state at a temperature on the order of 1 K. Figure 5 shows a comparison of the relative phase-space densities along the direction of the molecular beam $(z, v_z)$ of photostopped NO($^2\Pi_{3/2}, J = 1.5$) molecules in the source volume and the phase-space acceptance of the probe volume after 10 $\mu$s delay using experimentally measured or derived parameters. The thick black line represents the separatrix of the phase-space acceptance of a typical quadrupole trap made using permanent magnets with a trap depth of 1.3 K. To maximise the number of molecules that can be confined to such a trap, the phase-space emittance of the source should be matched to the acceptance of the trap. Figure 5(a) shows that the trap would not be deep enough to capture all of the photostopped molecules as many of the molecules have a $|v_z|$ that is outside the trap acceptance. Figure 5(b) shows that after 10 $\mu$s delay the velocity acceptance of the probe volume is well matched to that of the trap. Assuming that the dissociation laser can be made the same size as the trap, the estimated density after 10 $\mu$s delay can reasonably be expected to be the density of trapped molecules.

In order to minimise the number of molecules that would be lost from the trap due to the large velocity spread in the $x$ and $y$ directions, it may be possible to first pre-align the $NO_2$ molecules using an intense pulse of far off-resonance laser light [23]. Pre-alignment would have the effect of greatly increasing the anisotropy of the photofragments thus narrowing the $x$ and $y$ velocity spreads so that the phase-space emittance of the source will be better matched to the acceptance of the trap.

An advantage of the photostop technique is that any trap employed does not have to be opened to allow molecules to enter as the trappable molecules would be produced *in situ*. Multiple pulses of stopped molecules could therefore be accumulated to increase density in the trap. Several groups have proposed schemes for accumulating molecules in a trap. Meijer and co-workers are attempting to accumulate ground state NH molecules in a magnetostatic trap using a novel laser excitation scheme [24]. DeMille *et al.* have proposed that similar laser excitation schemes could be employed together with a buffer gas molecular beam technique to accumulate molecules in a microwave trap [25]. Raizen and co-workers have proposed that molecules can be cooled and accumulated in a RF-trap via the technique of single-photon cooling [26] and Rempe and co-workers have proposed a similar scheme to cool and accumulate molecules in a suitably tailored electric trap [27]. Chandler's kinematic cooling technique [28] is also capable, in principle, of accumulating molecules in a trap because, like photostop, the trappable molecules could be produced *in situ*. So far, trap accumulation has been demonstrated three times: Campbell *et al.* have used buffer gas cooling within a superconducting magnetostatic trap to accumulate ground state NH

molecules, although the trap lifetime is limited by the continued presence of the buffer gas [29]. In a variant of trap accumulation, Meijer and co-workers have loaded two distinct packets of ammonia molecules [30], and recently 19 distinct packets [31], into a molecular synchrotron.

The gain in density by accumulation of photostopped molecules in a trap will ultimately be limited by the balance between the trap loading rate and trap losses due to collisions with the "unused" parts of subsequent gas pulses. We have used a kinetic model to estimate the mean gain in density for the NO-Xe system considered here. Using conservative estimates of collision cross sections and parameters representing a well collimated, short gas pulse obtainable by beam chopping, the gain could, in principle, be in excess of one order of magnitude.

A suitable precursor for the photostop technique is a molecule that has a significant dissociation cross section at wavelengths that satisfy Equation (3) for typical molecular beam speeds. While $NO_2$ clearly satisfies this criterion, the bent nature of its $^2A_1$ ground and $^2B_2$ excited states favours rotational excitation of the NO fragment. This leads to a broad state distribution that dilutes the number of photostopped molecules and reduces the state selectivity of the technique. As mentioned earlier, oxygen atoms can also be stopped by the photodissociation of $NO_2$. However, by the same argument, $NO_2$ is not the most effective precursor. Polyatomic precursor molecules, where the photofragments on dissociation do not experience significant torques, are more favourable due to the small likelihood that the excess energy in the dissociation will be partitioned into rotational excitation of the molecular fragments. They are even more effective if they can be dissociated below the thresholds for vibrational excitation of the fragments. A precursor molecule that satisfies these criteria is nitrosyl cyanide (NCNO) as it is known to produce rotationally cold $CN(X\,^2\Sigma^+)$ radicals upon photodissociation close to threshold [32] and may also be a more efficient precursor for NO. The CN radical is an attractive species as it can be trapped magnetically and is a candidate molecule for single photon cooling [26]. It is known to undergo barrierless reactions, *e.g.* with $O_2$ [33], a species that has been Zeeman decelerated [12], thus making the CN + $O_2$ reaction a good system for ultracold chemistry. Effective precursors for producing photostopped atoms are likely to be diatomic molecules as the number of available electronic states is small given typical excess energies required for photostop [22].

## 6. Conclusions

Following the proof-of-principle experiments of Zhao *et al.* [19], we have shown that the peak of the velocity distribution of NO fragments, created by the photodissociation of $NO_2$ molecules in a supersonic beam, can be placed at zero velocity in the laboratory frame if the velocity cancellation condition is met exactly. Following a 10 $\mu$s period of evaporation, molecules are observed in the probe volume at an estimated density of *ca.* $10^7$ molecules cm$^{-3}$ per quantum state and a one-dimensional temperature of 1.3 K. By moving the photodissociation event closer to the nozzle, and employing beam chopping and precursor alignment techniques, it may be possible to increase the density by two orders of magnitude. The photostop technique is particularly suited towards trapping of molecules or atoms and offers the opportunity to accumulate them in a trap *in situ*. It may be ~~is~~ feasible to accumulate an order of magnitude more species compared to trap loading by a single shot. The experimental equipment and techniques employed are well established, thus making them accessible to many laboratories around the world that wish to perform experiments using slow molecules. With the right choice of precursor molecule, we believe that the photostop technique can complement existing techniques for slowing molecules and atoms and can add to the growing list of species that can be studied.



## Acknowledgements

We would like to thank the EPSRC for funding (GR/S22783/01 and EP/D055237/1). We also thank Miss Laura Harris, Mr Rob Rae and Mr Oliver Willis for their help. We also acknowledge Prof. Tim Softley for useful discussions and Prof. Jeremy Hutson for his scrutiny of the manuscript.

## References

[1] L.D. Carr, D. DeMille, R.V. Krems and J. Ye, Cold and ultracold molecules: science, technology and applicationsNew J. Phys. **11**, 055049 (2009).
[2] R.V. Krems, Phys. Chem. Chem. Phys. **10**, 4097 (2008).
[3] J.J. Hudson, B.E. Sauer, M.R. Tarbutt and E.A. Hinds, Phys. Rev. Lett. **89**, 023003 (2002).
[4] V.V. Flambaum and M.G. Kozlov, Enhanced sensitivity to the time variation of the fine-structure constant and mp/me in diatomic moleculesPhys. Rev. Lett. **99**, 150801 (2007).
[5] D. DeMille, Quantum computation with trapped polar moleculesPhys. Rev. Lett. **88**, 067901 (2002).

[6] A. Micheli, G.K. Brennen and P. Zoller, A toolbox for lattice-spin models with polar moleculesNature Phys. **2**, 341 (2006).
[7] K.K. Ni, S. Ospelkaus, M.H.G. de Miranda, A. Pe'er, B. Neyenhuis, J.J. Zirbel, S. Kotochigova, P.S. Julienne, D.S. Jin and J. Ye, Science **322**, 231 (2008).
[8] J.M. Sage, S. Sainis, T. Bergeman and D. DeMille, Phys. Rev. Lett. **94**, 203001 (2005).
[9] J. Deiglmayr, A. Grochola, M. Repp, K. Mörtlbauer, C. Glück, J. Lange, O. Dulieu, R. Wester and M. Weidemüller, Phys. Rev. Lett. **101**, 133004 (2008).
[10] E.S. Shuman, J.F. Barry and D. DeMille, Nature **467**, 820 (2010).
[11] A.O.G. Wallis and J.M. Hutson, Phys. Rev. Lett. **103**, 183201 (2009).
[12] E. Narevicius, A. Libson, C.G. Parthey, I. Chavez, J. Narevicius, U. Even and M.G. Raizen, Phys. Rev. A **77**, 051401 (2008).
[13] D. Patterson, J. Rasmussen and J.M. Doyle, New J. Phys. **11**, 055018 (2009).
[14] J.J. Kay, S.Y.T. van de Meerakker, K.E. Strecker and D.W. Chandler, Faraday Discuss. **142**, 143 (2009).
[15] M. Bell and T. Softley, Mol. Phys. **107**, 99 (2009).
[16] E. Tsikata, W.C. Campbell, M.T. Hummon, H.I. Lu and J.M. Doyle, New J. Phys. **12**, 065028 (2010).
[17] S.Y.T. van de Meerakker, H.L. Bethlem and G. Meijer, Nature Phys. **4**, 595 (2008).
[18] S.J. Matthews, S. Willitsch and T.P. Softley, Phys. Chem. Chem. Phys. **9**, 5656 (2007).
[19] B.S. Zhao, S.E. Shin, S.T. Park, X. Sun and D.S. Chung, J. Phys. Soc. Jpn. **78**, 094302 (2009).
[20] A.T.J.B. Eppink and D.H. Parker, Rev. Sci. Instr. **68**, 3477 (1997).
[21] R. Jost, J. Nygård, A. Pasinski and A. Delon, J. Chem. Phys. **105**, 1287 (1996).
[22] W.G. Doherty, M.T. Bell, T.P. Softley, A.M. Rowland, E. Wrede and D. Carty, Phys. Chem. Chem. Phys. (2010), submitted.
[23] J.J. Larsen, H. Sakai, C.P. Safvan, W.L. I. and S. H., J. Chem. Phys. **111**, 7774 (1999).
[24] S.Y.T. van de Meerakker, I. Labazan, S. Hoekstra, J. Küpper and G. Meijer, J. Phys. B **39**, S1077 (2006).
[25] D. DeMille, D. Glenn and J. Petricka, Eur. Phys. J. D **31**, 375 (2004).
[26] E. Narevicius, S. Travis Bannerman and M.G. Raizen, New J. Phys. **11**, 055046 (2009).
[27] M. Zeppenfeld, M. Motsch, P.W.H. Pinkse and G. Rempe, Phys. Rev. A **80**, 041401 (2009).
[28] E.W. Strecker and D.W. Chandler, Phys. Rev. A **78**, 063406 (2008).
[29] W.C. Campbell, E. Tsikata, H.I. Lu, L.D. van Buuren and J.M. Doyle, Phys. Rev. Lett. **98**, 213001 (2007).
[30] C.E. Heiner, D. Carty, G. Meijer and H.L. Bethlem, Nature Phys. **3**, 115 (2007).
[31] P.C. Zieger, S.Y.T. van de Meerakker, C.E. Heiner, H.L. Bethlem, A.J.A. van Roij and G. Meijer, Phys. Rev. Lett. **105**, 173001 (2010).
[32] I. Nadler, H. Reisler, M. Noble and C. Wittig, J. Chem. Phys. **82**, 2608 (1985).
[33] I.R. Sims, J.L. Queffelec, A. Defrance, C. Rebrion-Rowe, D. Travers, B.R. Rowe and I.W.M. Smith, J. Chem. Phys. **97**, 8798 (1992).